

This discussion paper is/has been under review for the journal *Atmospheric Chemistry and Physics (ACP)*. Please refer to the corresponding final paper in *ACP* if available.

**Experimental error  
and air-sea gas  
exchange**

W. E. Asher

# The effects of experimental uncertainty in parameterizing air-sea gas exchange using tracer experiment data

W. E. Asher

University of Washington, Seattle, Washington

Received: 4 July 2008 – Accepted: 30 July 2008 – Published: 3 September 2008

Correspondence to: W. E. Asher (asher@apl.washington.edu)

Published by Copernicus Publications on behalf of the European Geosciences Union.

Title Page

Abstract

Introduction

Conclusions

References

Tables

Figures

◀

▶

◀

▶

Back

Close

Full Screen / Esc

Printer-friendly Version

Interactive Discussion



## Abstract

It is not practical to measure air-sea gas fluxes in the open ocean for all conditions and areas of interest. Therefore, in many cases fluxes are estimated from measurements of air-phase and water-phase gas concentrations, a measured environmental forcing function such as wind speed, and a parameterization of the air-sea transfer velocity in terms of the environmental forcing function. One problem with this approach is that when direct measurements of the transfer velocity are plotted versus the most commonly used forcing function, wind speed, there is considerable scatter, leading to a relatively large uncertainty in the flux. Because it is known that multiple processes can affect gas transfer, it is commonly assumed that this scatter is caused by single-forcing function parameterizations being incomplete in a physical sense. However, scatter in the experimental data can also result from experimental uncertainty (i.e., measurement error). Here, results from field and laboratory results are used to estimate how experimental uncertainty contributes to the observed scatter in the measured fluxes and transfer velocities as a function of environmental forcing. The results show that experimental uncertainty could explain a major portion of the observed scatter in field and laboratory measurements of the air-sea gas transfer velocity.

## 1 Introduction

Advances in techniques for measuring air-sea fluxes have resulted in several new oceanic data sets of oceanic gas fluxes. In addition, novel experimental methodologies and detailed microphysical process studies have provided new information concerning the fundamental mechanisms controlling air-water gas exchange. These field and laboratory data have been used in developing and testing air-sea gas exchange dependencies and have allowed commonly used conceptual models to be tested. However, even with the advances in the understanding of the process and the additional experimental capabilities, variability in both laboratory and field data as a function of

### Experimental error and air-sea gas exchange

W. E. Asher

Title Page

Abstract

Introduction

Conclusions

References

Tables

Figures

◀

▶

◀

▶

Back

Close

Full Screen / Esc

Printer-friendly Version

Interactive Discussion



a particular variable characterizing the major forcing functions (e.g., wind stress) has made development of a robust method for parameterizing the gas transfer velocity difficult.

In general, the air-sea flux of a sparingly soluble non-reactive gas at low to moderate wind speeds can be written as the product of a kinetic term, the air-sea gas transfer velocity  $k_L$  ( $\mu\text{m s}^{-1}$ ), and a thermodynamic driving force defined in terms of the disequilibrium in chemical potential of the gas between the ocean and the atmosphere. This driving force is commonly expressed in terms of the air-water partial pressure difference,  $\Delta P$  (kPa) assuming that most gases of interest will behave ideally so that the fugacity in each phase is equal to their partial pressure in that phase. Although there is some evidence that errors in  $\Delta P$  can affect the measurement of  $k_L$  (Jacobs et al., 2002), this is by no means conclusive and this discussion will focus on the kinetic term  $k_L$ .

It is well understood that in the absence of bubbles  $k_L$  depends on both the molecular diffusivity,  $D$  ( $\text{m}^2 \text{s}^{-1}$ ), of the gas in the aqueous phase and on the water-side turbulence very close to the free surface (Davies, 1972). However, the details of these dependencies as they relate to the particulars of gas transfer at the ocean surface are not well known and still subject to considerable debate. For example, it is clear that the presence of naturally occurring surface active material (which will be referred to here as “surfactants” for short) can inhibit air-water gas transfer (Frew et al., 1990). However, it is less clear that field measurements of  $k_L$  can be easily partitioned into those made under surfactant-impacted conditions and those made under so-called clean conditions. Even more uncertain is how to best parameterize the role of turbulence in influencing the magnitude of  $k_L$ .

Under most conditions, the wind stress plays a dominant role in providing the turbulent kinetic energy involved in promoting gas exchange. Therefore, wind speed,  $U$ , has long been used to parameterize  $k_L$ . Figure 1 shows  $k_L$  measured in the ocean using the purposeful dual-tracer method (Wanninkhof et al., 1993) plotted as a function of  $U$  (the data in the figure were compiled from Wanninkhof et al., 1993, 1997, 2004; Jacobs et al., 1999; Nightingale et al., 2000a, b; and Ho et al., 2006 and have all been scaled

---

## Experimental error and air-sea gas exchange

W. E. Asher

---

Title Page

Abstract

Introduction

Conclusions

References

Tables

Figures

◀

▶

◀

▶

Back

Close

Full Screen / Esc

Printer-friendly Version

Interactive Discussion



**Experimental error  
and air-sea gas  
exchange**

W. E. Asher

Title Page

Abstract

Introduction

Conclusions

References

Tables

Figures

◀

▶

◀

▶

Back

Close

Full Screen / Esc

Printer-friendly Version

Interactive Discussion

to a common diffusivity equal to carbon dioxide in seawater at 293.15 K, defined here in terms of the Schmidt number (660), assuming that  $k_L$  is proportional to  $D^{1/2}$ ). When the values for the scaled transfer velocity,  $k_{660}$ , at a particular  $U$  are compared, the data are considerably scattered. It can be argued that the overall dependence follows either a polynomial dependence or a segmented linear dependence with  $U$ . Unfortunately, there is too much scatter in the data to allow the data to provide a definitive selection between any of the available gas exchange parameterizations.

Figure 1 typifies the problem in attempting to develop a method for accurately estimating  $k_L$  from an easily measured environmental parameter. The data in the figure represent measurements of the highest quality, collected by meticulous and careful groups. Because of this, it is assumed that much of the scatter in the data represents variability in the transfer velocity imposed by variability in the environmental conditions. This could occur if, for example, the levels of aqueous-phase turbulence generated at a particular value of  $U$  depend on factors other than the  $U$  itself. This explanation seems logical on an intuitive level, but the fundamental measurements of near-surface oceanic turbulence necessary to support it are not available. So it could be that the scatter in Fig. 1 could simply represent experimental uncertainty rather than environmental variability.

The purpose of this paper is to explore whether it is possible to explain the scatter in various measurements of the  $k_L$  simply in terms of the uncertainty in measuring the underlying parameters. This will be done using the dual-tracer data shown in Fig. 1 and using gas transfer data collected in a wind-wave tunnel.

## 2 Theory

In the case where a non-reactive gaseous tracer is injected into a known volume of water, the change in concentration with respect to time due to the water-to-air gas flux

can be written as

$$\frac{dC_B}{dt} = \frac{k_L A}{V} (K_H P_A - C_B) \quad (1)$$

where  $C_B$  is the bulk-phase concentration of the tracer gas ( $\text{mol m}^{-3}$ ),  $A$  is the surface area of the water through which gas exchange occurs ( $\text{m}^2$ ),  $V$  is the total water volume ( $\text{m}^3$ ),  $K_H$  is the aqueous-phase solubility of the gas ( $\text{mol m}^{-3} \text{kPa}^{-1}$ ), and  $P_A$  is the partial pressure of the gas in the air phase (kPa). Integration of Eq. (1) shows that  $k_L$  can be written as

$$k_L = \frac{V}{A \Delta t} \ln \left( \frac{C_S - C_0}{C_S - C_B} \right) \quad (2)$$

where  $\Delta t$  is the time difference and  $C_0$  is the concentration of the tracer gas at time  $t=0$ . From Eq. (2), a plot of the quantity  $-\ln((C_S - C_0)/(C_S - C_B))$  versus time will result in a straight line with slope equal to  $k_L A/V$ .

A similar relation exists for the analysis of purposeful dual-tracer method (PDTM) data collected during oceanic air-sea gas exchange measurements. In these experiments, the two volatile tracer gases sulfur hexafluoride ( $\text{SF}_6$ ) and helium-3 ( $^3\text{He}$ ) are injected into the surface mixed layer. Their concentrations are then measured as a function of time and the transfer velocity of  $^3\text{He}$ ,  $k_L(^3\text{He})$ , can be estimated from the change in the concentration ratio of the two tracers. This relation has the form

$$k_L(^3\text{He}) = \frac{-h}{\Delta t} \Delta \left\{ \ln \left( \frac{[^3\text{He}]}{[\text{SF}_6]} \right) \right\} \left\{ 1 - \left[ \frac{\text{Sc}(^3\text{He})}{\text{Sc}(\text{SF}_6)} \right]^{1/2} \right\}^{-1} \quad (3)$$

where  $h$  is the mixed layer depth,  $\Delta t$  is the time interval over which the change in concentrations are measured,  $[^3\text{He}]$  and  $[\text{SF}_6]$  are the concentrations of  $^3\text{He}$  and  $\text{SF}_6$ , respectively, and  $\text{Sc}(^3\text{He})$  and  $\text{Sc}(\text{SF}_6)$  are the Schmidt numbers of  $^3\text{He}$  and  $\text{SF}_6$ , respectively.

**Experimental error  
and air-sea gas  
exchange**

W. E. Asher

Title Page

Abstract

Introduction

Conclusions

References

Tables

Figures

◀

▶

◀

▶

Back

Close

Full Screen / Esc

Printer-friendly Version

Interactive Discussion



## Experimental error and air-sea gas exchange

W. E. Asher

Title Page

Abstract

Introduction

Conclusions

References

Tables

Figures

◀

▶

◀

▶

Back

Close

Full Screen / Esc

Printer-friendly Version

Interactive Discussion



Applying either Eq. (2) or Eq. (3) is straightforward and the theoretical basis for either is not in dispute (with possible exception being the correct value of the exponent for the Schmidt number term). However, because of the logarithmic relationship involving the concentrations and the fact that the change in concentration with respect to time can be relatively small, both equations are sensitive to measurement uncertainty.

In laboratory experiments, it is common to simultaneously measure  $k_L$  for several gases. From these data, it is possible to estimate the dependence of  $k_L$  on molecular diffusivity. Conceptual models for air-water gas transfer assume that this dependence can be written as

$$k_L = a \left( \frac{\nu}{D} \right)^{-n} f(Q, L) \quad (4)$$

where  $a$  and  $n$  are constants,  $\nu$  is the kinematic viscosity of water, and  $f(Q, L)$  symbolizes the as yet unspecified dependence of  $k_L$  on the turbulence velocity and length scales. The ratio  $\nu/D$  is the Schmidt number,  $Sc$ , and it will be used from this point in place of  $D$ . Depending on the conceptual model,  $n$  can range from 1/2 to 2/3 with the lower value usually associated with gas exchange through a clean water surface and higher values associated with transfer through surfactant influenced surfaces. Therefore, the dependence of  $k_L$  on  $Sc$  provides very useful information on the transfer process and it is highly desirable to be able to estimate  $n$  from experimental data.

Using Eq. (4), it can be shown that if the  $k_L$  values for two gases with different  $Sc$  numbers are known,  $n$  is equal to

$$n = \frac{\ln [k_L(1) / k_L(2)]}{\ln [Sc(2) / Sc(1)]} \quad (5)$$

where the (1) and (2) refer to the parameter for the two respective gases. As is the case for calculating  $k_L$  itself, Eq. (5) is also sensitive to measurement errors because  $Sc$  for most gases does not vary by a large amount.

### 3 Wind-wave tunnel measurements

The Flux Exchange Dynamics Study (FEDS) was conducted in 1998 at the Air-Sea Interaction Research Facility (ASIRF) wind-wave tunnel at the US National Aeronautics and Space Agency, Goddard Space Flight Center, Wallops Flight Facility in Wallops Island, Virginia. These measurements have been described in detail elsewhere (Zappa et al., 2004) and only a brief description will be provided here. During the study,  $k_L$  was measured for SF<sub>6</sub> and helium (He) using gas chromatography to determine aqueous-phase gas concentrations. Method precision for gas concentrations was found to be ±3% for SF<sub>6</sub> and ±7% for He. Figure 2 shows transfer velocities for He normalized to Sc=660 assuming  $n=1/2$ ,  $k_{660}(\text{He})$ , measured during FEDS plotted as a function of wind speed,  $U$ . Figure 3 shows transfer velocities measured during FEDS for SF<sub>6</sub> normalized to Sc=660,  $k_{660}(\text{SF}_6)$ , also plotted versus  $U$ . Sc values for SF<sub>6</sub> were taken from King and Saltzman (1995) and Sc for He was taken from Wanninkhof (1992).

As was seen in the field data in Fig. 1, there is some scatter in the measured values of the transfer velocity when plotted versus  $U$ . However, in contrast to the field data,  $k_L$  in the wind-wave tunnel increases approximately linearly with  $U$ . What is not clear from the data is whether the scatter in  $k_L$  reflect experimental noise or day-to-day variability in the conditions affecting gas transfer in the wind tunnel. In order to understand the relative roles experimental uncertainty and environmental variability play in governing the scatter in measured  $k_L$  values, a Monte Carlo-type simulation was performed using the known experimental uncertainties to estimate the variability in  $k_L$  that would be expected given the uncertainties in the gas concentrations.

The first step in this procedure was to use the experimental data in Figs. 2 and 3 to produce a linear relation for estimating  $k_L$  from wind speed in the ASIRF wind-wave tunnel. Least-squares linear regression of the combined gas transfer data set showed that  $k_L$  at a particular value of Sc,  $k_L(\text{Sc})$ , could be calculated as

$$k_L(\text{Sc}) = \left(\frac{660}{\text{Sc}}\right)^{1/2} (6.73 U - 10.76) \quad (6)$$

## Experimental error and air-sea gas exchange

W. E. Asher

Title Page

Abstract

Introduction

Conclusions

References

Tables

Figures

◀

▶

◀

▶

Back

Close

Full Screen / Esc

Printer-friendly Version

Interactive Discussion



for  $k_L(\text{Sc})$  in  $\mu\text{m s}^{-1}$  and  $U$  in  $\text{m s}^{-1}$  with the coefficient of determination for the regression being 0.91 and a standard error of the fit equal to  $5.29 \mu\text{m s}^{-1}$ . Then, Eq. (2) was rewritten in the form

$$C_B = C_B - (C_S - C_0) \exp\left(-\frac{A k_L(\text{Sc}) t}{V}\right) \quad (7)$$

so that gas concentrations for a gas with a particular Schmidt number could be predicted as a function of  $t$ . Concentrations for He and  $\text{SF}_6$  were predicted at five times with time steps on the order of 2000 s so that the number of modeled concentrations and their time steps were equal to the experimental sampling rate. Then, the predicted concentrations were modified by adding or subtracting a random amount determined by the measurement error for that particular gas. For the Monte Carlo simulations, 1000 separate sets of concentrations with independent experimental uncertainties were produced for each gas at  $U = 4 \text{ m s}^{-1}$ ,  $6 \text{ m s}^{-1}$ ,  $8 \text{ m s}^{-1}$ ,  $10 \text{ m s}^{-1}$ , and  $12 \text{ m s}^{-1}$ . These concentrations were then used in Eq. (2) to calculate  $k_{660}(\text{SF}_6)$  and  $k_{660}(\text{He})$ . The mean value of the model-calculated transfer velocities,  $k_{660}(\text{He})_{\text{AVG}}$  and  $k_{660}(\text{SF}_6)_{\text{AVG}}$ , are shown in Figs. 2 and 3, respectively. Also shown in each figure are  $k_{660}(\text{He})_{\text{AVG}} \pm 2\sigma_{\text{He}}$  and  $k_{660}(\text{SF}_6)_{\text{AVG}} \pm 2\sigma_{\text{SF}_6}$ , or the bounds showing range of approximately 90% of the model-derived  $k_L$  values (i.e., approximately 900 out of the 1000 calculated transfer velocities lie within the dashed lines in each figure).

The range of the modeled transfer velocities at a given wind speed span the observed experimental scatter at all wind speeds. This indicates that the variability in the data is primarily due to concentration measurement precision and not day-to-day changes in uncharacterized environmental conditions in the wind-wave tunnel.

The modeled concentrations can also be used to study the variability in values of  $n$  deduced from measurements of  $k_L$ . Figure 4 shows  $n$  calculated using Eq. (5) and  $k_L(\text{SF}_6)$  and  $k_L(\text{He})$  measured in the wind-wave tunnel plotted vs.  $U$ . Also shown in Fig. 4 is the average Schmidt number exponent,  $n_{\text{AVG}}$ , calculated using the gas transfer velocities calculated from the Monte Carlo simulation above and Eq. (5). As expected

**Experimental error  
and air-sea gas  
exchange**

W. E. Asher

Title Page

Abstract

Introduction

Conclusions

References

Tables

Figures

◀

▶

◀

▶

Back

Close

Full Screen / Esc

Printer-friendly Version

Interactive Discussion





## Experimental error and air-sea gas exchange

W. E. Asher

Title Page

Abstract

Introduction

Conclusions

References

Tables

Figures

◀

▶

◀

▶

Back

Close

Full Screen / Esc

Printer-friendly Version

Interactive Discussion



for a clean surface,  $n_{\text{AVG}}=1/2$ . Of more interest is the range in  $n_{\text{AVG}}$ , here expressed as  $n_{\text{AVG}}\pm 2\sigma_n$  where  $\sigma_n$  is the standard deviation of the 1000  $n$  values from the Monte Carlo simulation. The range in  $n_{\text{AVG}}\pm 2\sigma_n$  spans the variability in  $n$  calculated from the wind-tunnel data. This suggests that the variability observed in Fig. 4 is not due to environmental variability and merely reflects the sensitivity of  $n$  to the experimental uncertainty in calculating  $k_L$ .

In the above analysis of the variability in  $n$ , it was assumed that  $n$  was equal to 1/2 and constant as a function of wind speed. However, laboratory data exists suggesting that  $n$  is a function of  $U$ , decreasing from 2/3 to 1/2 as  $U$  increases (Jähne et al., 1984; Zappa et al., 2004). Since understanding the dependence of  $k_L$  on  $n$  is important in determining a correct conceptual model for air-water gas transfer (Atmane et al., 2004) and in analyzing results from oceanic dual-tracer gas exchange experiments, it is often the case that gas transfer measurements are used to determine the dependence of  $n$  on wind speed.

The Monte Carlo method described above was used to assess how measurement errors might affect determining the functionality of  $n$  with respect to  $U$ . First, it was assumed that  $n$  was given by

$$\begin{aligned} n=0.67: & \quad U < 2 \text{ m s}^{-1} \\ n=0.5+0.17 \exp\left(\frac{U-2}{2}\right): & \quad U \geq 2 \text{ m s}^{-1} \end{aligned} \quad (8)$$

and then  $k_L$  values were calculated for the gases methane ( $\text{CH}_4$ ),  $\text{SF}_6$ , and He using Eq. (6) using  $n$  calculated using Eq. (8) in place of the exponent 1/2. Sc values for  $\text{CH}_4$  were taken from Wanninkhof (1992). Transfer velocities were calculated at  $U=3 \text{ m s}^{-1}$ ,  $4 \text{ m s}^{-1}$ ,  $6 \text{ m s}^{-1}$ ,  $8 \text{ m s}^{-1}$ ,  $10 \text{ m s}^{-1}$ , and  $12 \text{ m s}^{-1}$ . As before, 1000 concentration time series that included a  $\pm 3\%$  random error and had time steps as given above in each value were generated for each gas. Then,  $k_L$  was calculated using each concentration time series. An estimate of  $n$  could then be derived using the gas pairs  $\text{CH}_4/\text{SF}_6$ ,  $\text{CH}_4/\text{He}$ , and  $\text{SF}_6/\text{He}$ . Figure 5 shows  $n_{\text{AVG}}$  and  $n_{\text{AVG}}\pm 2\sigma_n$  for all three gas pairs.

The top panel in Fig. 5 shows the results for  $\text{CH}_4/\text{SF}_6$ . Because the change in

Sc value for these two gases is relatively small (e.g.,  $Sc(CH_4)=616$  at 293.15 K,  $Sc(SF_6)=948$  at 293.15 K), the calculation of  $n$  is very sensitive to measurement error so the  $\pm 2\sigma_n$  range is large and if only a few experiments were conducted, it is doubtful the functionality of  $n$  given by Eq. (8) would result. The situation improves for both gas pairs involving He, mainly because  $Sc(He)=149$  at 293.15 K. However, the variability in the calculated  $n$  values is still large and accurately resolving the dependence of  $n$  on wind speed would require a significant number of experiments be conducted.

#### 4 Oceanic purposeful dual-tracer measurements

The Monte Carlo method described in the previous section can also be applied to the purposeful dual-tracer method (PDTM). However, in the case of PDTM data analysis, in addition to the measurement uncertainties in the gas concentrations, the uncertainty in the mixed layer depth,  $h$ , must also be taken into account. As discussed by Wanninkhof et al. (2004), the analysis of PDTM data proceeds by analyzing discrete segments of a times series of concentrations for the two gases over intervals where the wind speed was relatively constant. Rather than address the effect of averaging wind speed, which has been discussed in some detail elsewhere (Wanninkhof et al., 2004), here the effect of measurement variability under steady winds will be studied.

For the simulations performed here, it was assumed that the concentrations of both  $SF_6$  and  $^3He$  could be measured in the ocean with a precision of  $\pm 2\%$  (R. Wanninkhof, NOAA Atlantic Oceanographic and Meteorological Laboratory, Miami Florida, personal communication, 2007). Defining the uncertainty in  $h$  is more problematic, and it was assumed to be  $\pm 20\%$  based on the uncertainty in extracting the mixed-layer depth from CTD profiles (D. Ho, Lamont Doherty Earth Observatory, Palisades New York, personal communication, 2007). Given the large difference in precisions, it is was found that uncertainty in  $h$  has the largest effect on  $k_L(^3He)$ .

Unfortunately, the precision in gas concentration analysis for the oceanic dual-tracer data is different than the precision in concentration analysis for the wind-tunnel data

### Experimental error and air-sea gas exchange

W. E. Asher

Title Page

Abstract

Introduction

Conclusions

References

Tables

Figures

◀

▶

◀

▶

Back

Close

Full Screen / Esc

Printer-friendly Version

Interactive Discussion



discussed above. This makes direct comparison of the data problematic, but because of differences in instrumentation and analytical techniques, it is not correct to use the same experimental precisions for each set of experiments.

The Monte Carlo simulations were carried out by calculating the transfer velocities of SF<sub>6</sub> and He,  $k_L(\text{SF}_6)$  and  $k_L(\text{He})$ , respectively, at for  $U=4\text{ m s}^{-1}$ ,  $8\text{ m s}^{-1}$ ,  $12\text{ m s}^{-1}$  and  $16\text{ m s}^{-1}$  using the  $U^2$  power law dependence proposed by Wanninkhof (1992). Assuming that  $h=50\text{ m}$  (and that  $A/V=1/h$ ) allowed Eq. (7) to be used with these  $k_L$  values to generate concentrations for SF<sub>6</sub> and <sup>3</sup>He at discrete times. Concentration pairs were calculated at  $t=0$  and at times with  $\Delta t$  in the range of 1–2 days. These concentrations were used in Eq. (3) to calculate  $k_L(^3\text{He})$ . As was done previously, 1000 sets of concentrations were generated at each  $U$  and a mean transfer velocity normalized to  $Sc=660$ ,  $k_{660}(^3\text{He})_{\text{AVG}}$ , and associated standard deviation,  $\sigma_{^3\text{He}}$ , were calculated. Figure 6 shows the data from Figure 1 along with the  $k_{660}(^3\text{He})_{\text{AVG}}$ , and the range of the model results given as  $k_{660}(\text{He})_{\text{AVG}} \pm 2\sigma_{^3\text{He}}$ . Of the 37 field data points, 21 fall in the range of the modeled transfer velocities. The fraction of points falling in the model range represents an estimate of the variability in the measured PDTM transfer velocities that is due to measurement errors. Therefore, these results indicate that approximately 60% observed variability in the results is due to uncertainty in gas concentration measurements and knowledge of the depth of the mixed layer. This suggests that environmental variability may not play as large a role as supposed, and that mixed-layer depth in particular is a critical parameter in analysis of PDTM results.

## 5 Conclusions

The simple Monte Carlo model used here does not account for all sources of experimental variability in measuring air-water gas transfer velocities. However, it is instructive that using realistic values for the uncertainties in the concentration measurements and estimations of the mixed layer depth, much of the observed variability in transfer velocities measured in wind-wave tunnels and in the ocean can be explained. This

### Experimental error and air-sea gas exchange

W. E. Asher

Title Page

Abstract

Introduction

Conclusions

References

Tables

Figures

◀

▶

◀

▶

Back

Close

Full Screen / Esc

Printer-friendly Version

Interactive Discussion



suggests that in both the field and laboratory there is less variability in the forcing mechanisms driving gas exchange than previously thought and that perhaps the overall pattern of the data in Fig. 6 is somewhat close to the “true” functional dependence of  $k_L$  on wind speed. In turn, this is relatively good news for those who hope to develop a robust method for parameterizing gas transfer in terms of an easily measured environmental variable. However, it also points out the difficulty associated with making the measurements used to validate these parameterizations, especially in regards to determining the functional dependence of  $k_L$  on Schmidt number.

*Acknowledgements.* This work was funded by the National Science Foundation under grant OCE-0425305.

## References

- Atmane, M. A., Asher, W. E., and Jessup, A. T.: On the use of the active infrared technique to infer heat and gas transfer velocities at the air-water free surface, *J. Geophys. Res.*, 109, C08S14, doi:10.1029/2003JC001805, 2004.
- Davies, J. T.: Turbulence phenomena: an introduction to the Eddy Transfer of momentum, mass, and heat, particularly at interfaces, Academic Press, New York, USA, 1972.
- Frew, N. M., Goldman, J. C., Dennett, M. R., and Johnson, A. S.: Impact of phytoplankton-generated surfactants on air-sea gas exchange, *J. Geophys. Res.*, 95, 3337–3352, 1990.
- Ho, D. T., Law, C. S., Smith, M. J., Schlosser, P., Harvey, M., and Hill, P.: Measurements of air-sea gas exchange at high wind speeds in the Southern Ocean: Implications for global parameterizations, *Geophys. Res. Lett.*, 33, L16611, doi:10.1029/2006GL026817, 2006.
- Jacobs, C., Kjeld, J. F., Nightingale, P., Upstill-Goddard, R., Larsen, S., and Oost, W.: Possible errors in CO<sub>2</sub> air-sea transfer velocity from deliberate tracer releases and eddy covariance measurements due to near-surface concentration gradients, *J. Geophys. Res.-Oceans* 107(C9), 3128, doi:10.1029/2001JC000983, 2002.
- Jacobs, C. M. J., Kohsiek, W., and Oost, W. A.: Air-sea fluxes and transfer velocity of CO<sub>2</sub> over the North Sea: results from ASGAMAGE, *Tellus B*, 51, 629–641, 1999.
- Jähne, B., Huber, W., Dutzi, A., Wais, T., and Illmerger, J.: Wind/wave tunnel experiments on the Schmidt number and wave field dependence of air-water gas exchange, in: *Gas* 16704

## Experimental error and air-sea gas exchange

W. E. Asher

Title Page

Abstract

Introduction

Conclusions

References

Tables

Figures

◀

▶

◀

▶

Back

Close

Full Screen / Esc

Printer-friendly Version

Interactive Discussion



Transfer at Water Surfaces, edited by: Brutsaert, W. and Jirka, G. H., Reidel, Dordrecht, The Netherlands, 303–310, 1984.

King, D. B. and Saltzman, E. S.: Measurement of the diffusion coefficient of sulfur hexafluoride in water, *J. Geophys. Res.*, 100, 7083–7088, 1995.

5 Nightingale, P. D., Liss, P. S., and Schlosser, P.: Measurements of air-sea gas transfer during an open ocean algal bloom, *Geophys. Res. Lett.*, 27(14), 2117–2120, 2000a.

Nightingale, P. D., Malin, G., Law, C. S., Watson, A. J., Liss, P. S., Liddicoat, M. I., Boutin, J., and Upstill-Goddard, R. C.: In situ evaluation of air-sea gas exchange parameterizations using novel conservative and volatile tracers, *Global Biogeochem. Cy.*, 14, 373–387, 2000b.

10 Wanninkhof, R.: Relationship between wind speed and gas exchange over the ocean, *J. Geophys. Res.*, 97, 7373–7382, 1992.

Wanninkhof, R., Asher, W. E., Weppernig, R., Chen, H., Schlosser, P., Langdon, C., and Sambrotto, R.: Gas transfer experiment on Georges Bank using two volatile deliberate tracers, *J. Geophys. Res.*, 98, 20237–20248, 1993.

15 Wanninkhof, R., Hitchcock, G., Wiseman, W., Ortner, P., Asher, W., Ho, D., Schlosser, P., Dickson, M.-L., Anderson, M., Masserini, R., Fanning, K., and Zhang, J.-Z.: Gas exchange, dispersion, and biological productivity on the west Florida shelf: Results from a Lagrangian tracer study, *Geophys. Res. Lett.*, 24, 1767–1770, 1997.

Wanninkhof, R., Sullivan, K. F., and Top, Z.: Air-sea gas transfer in the Southern Ocean, *J. Geophys. Res.-Oceans* 109, C08S19, doi:10.1029/2003JC001767, 2004.

20 Zappa, C. J., Asher, W. E., Jessup, A. T., Klinke, J., and Long, S. R.: Microbreaking and the enhancement of air-water gas transfer velocities, *J. Geophys. Res.*, 109, C08S16, doi:10.1029/2003JC001897, 2004.

ACPD

8, 16693–16711, 2008

---

## Experimental error and air-sea gas exchange

W. E. Asher

---

Title Page

Abstract

Introduction

Conclusions

References

Tables

Figures

◀

▶

◀

▶

Back

Close

Full Screen / Esc

Printer-friendly Version

Interactive Discussion



**Experimental error  
and air-sea gas  
exchange**

W. E. Asher

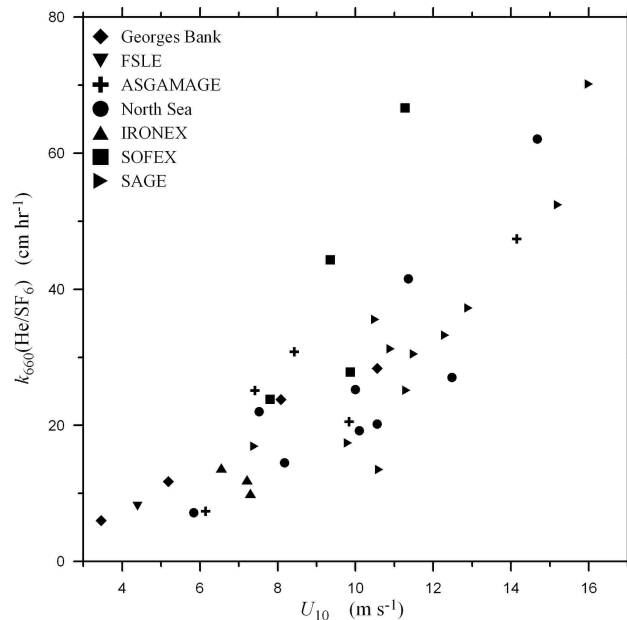


**Fig. 1.** Available oceanic measurements of the air-sea gas transfer velocity made using the purposeful dual-tracer method normalized to a common Schmidt number of 660,  $k_{660}(\text{He})$ , plotted as a function of wind speed. The data key is shown on the figure. In the key: Georges Bank is data from Wanninkhof et al. (1993); FSLE is data from Wanninkhof et al. (1997); ASGAMAGE is data from Jacobs et al. (1999); North Sea is data from Nightingale et al. (2000b), IRONEX is data from Nightingale et al. (2000a); SOFEX is data from Wanninkhof et al. (2004); and SAGE is data from Ho et al. (2006).

[Title Page](#)[Abstract](#)[Introduction](#)[Conclusions](#)[References](#)[Tables](#)[Figures](#)[◀](#)[▶](#)[◀](#)[▶](#)[Back](#)[Close](#)[Full Screen / Esc](#)[Printer-friendly Version](#)[Interactive Discussion](#)

**Experimental error  
and air-sea gas  
exchange**

W. E. Asher

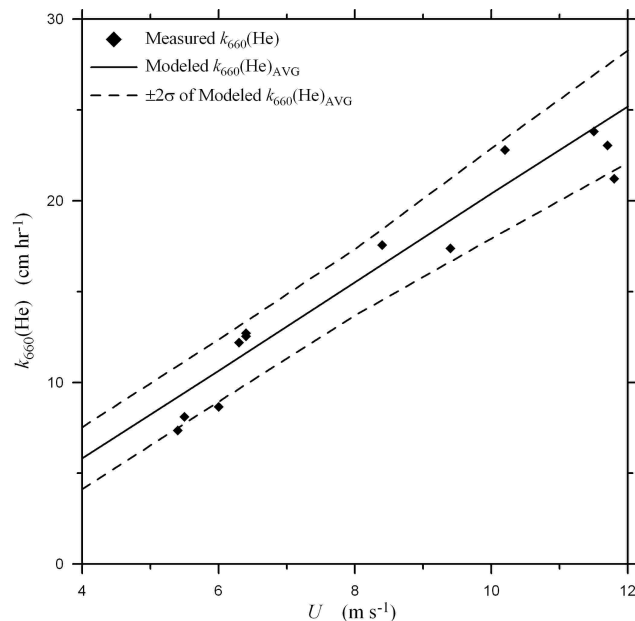


**Fig. 2.** The air-water gas transfer velocity for He normalized to  $Sc=660$ ,  $k_{660}(\text{He})$ , measured during FEDS plotted as a function of wind speed. Also shown are values for  $k_{660}(\text{He})$  produced by the Monte Carlo model described in Sect. 3. The data key is shown on the figure. The dashed lines represent the values bounding 90% of the  $k_{660}(\text{He})$  values produced by the Monte Carlo model.

Title Page

Abstract

Introduction

Conclusions

References

Tables

Figures

◀

▶

◀

▶

Back

Close

Full Screen / Esc

Printer-friendly Version

Interactive Discussion



**Experimental error  
and air-sea gas  
exchange**

W. E. Asher

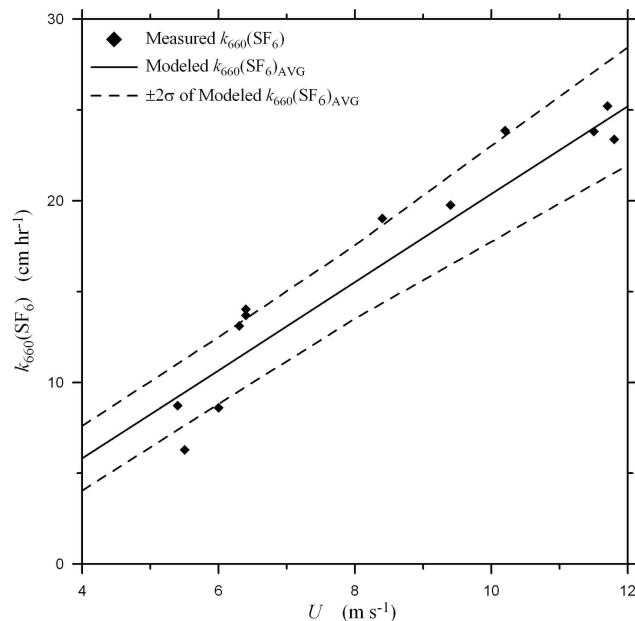


**Fig. 3.** The air-water gas transfer velocity for  $\text{SF}_6$  normalized to  $\text{Sc}=660$ ,  $k_{660}(\text{SF}_6)$ , measured during FEDS plotted as a function of wind speed. Also shown are values for  $k_{660}(\text{SF}_6)$  produced by the Monte Carlo model described in Sect. 3. The data key is shown on the figure. The dashed lines represent the values bounding 90% of the  $k_{660}(\text{SF}_6)$  values produced by the Monte Carlo model.

[Title Page](#)[Abstract](#)[Introduction](#)[Conclusions](#)[References](#)[Tables](#)[Figures](#)[◀](#)[▶](#)[◀](#)[▶](#)[Back](#)[Close](#)[Full Screen / Esc](#)[Printer-friendly Version](#)[Interactive Discussion](#)



## Experimental error and air-sea gas exchange

W. E. Asher

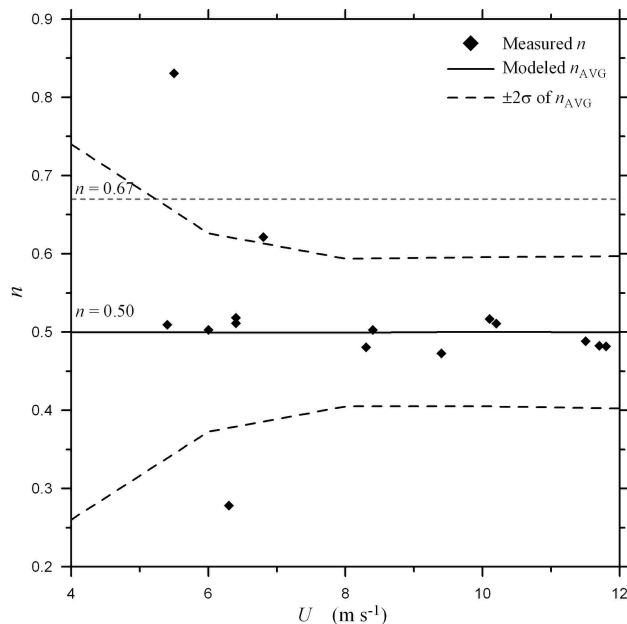


**Fig. 4.** The Schmidt number exponent,  $n$ , calculated using Eq. (5) and gas transfer velocity data for the gas pair  $\text{SF}_6$  and He measured in the Wallops Flight Facility wind/wave tunnel. Also shown in the figure is the average  $n$ ,  $n_{AVG}$ , and range of  $n$  calculated using the Monte Carlo method and 1000 trial runs. The data key is shown on the figure where  $\sigma$  is the standard deviation of the modeled  $n$  values.

Title Page

Abstract

Introduction

Conclusions

References

Tables

Figures

◀

▶

◀

▶

Back

Close

Full Screen / Esc

Printer-friendly Version

Interactive Discussion



Experimental error  
and air-sea gas  
exchange

W. E. Asher

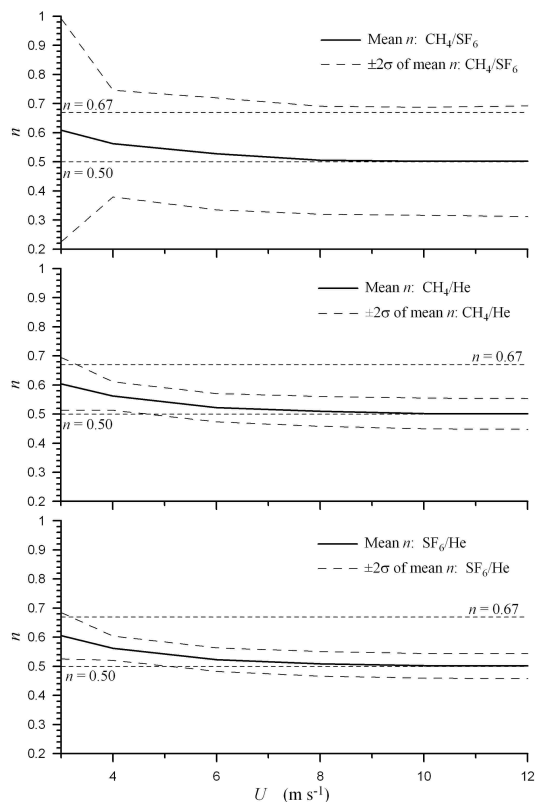


**Fig. 5.** Plots of the expected experimental variance in Sc exponent  $n$  calculated using Eq. (5) and transfer velocities from the Monte Carlo procedure described in the text plotted as a function of wind speed,  $U$ , for the gas pairs: methane (CH<sub>4</sub>) and sulfur hexafluoride (SF<sub>6</sub>), top panel; CH<sub>4</sub> and helium (He), middle panel; and He and SF<sub>6</sub>, bottom panel. The model assumes the uncertainties in gas concentrations are uncorrelated. The data key for each is shown on each figure.

[Title Page](#)[Abstract](#)[Introduction](#)[Conclusions](#)[References](#)[Tables](#)[Figures](#)[◀](#)[▶](#)[◀](#)[▶](#)[Back](#)[Close](#)[Full Screen / Esc](#)[Printer-friendly Version](#)[Interactive Discussion](#)

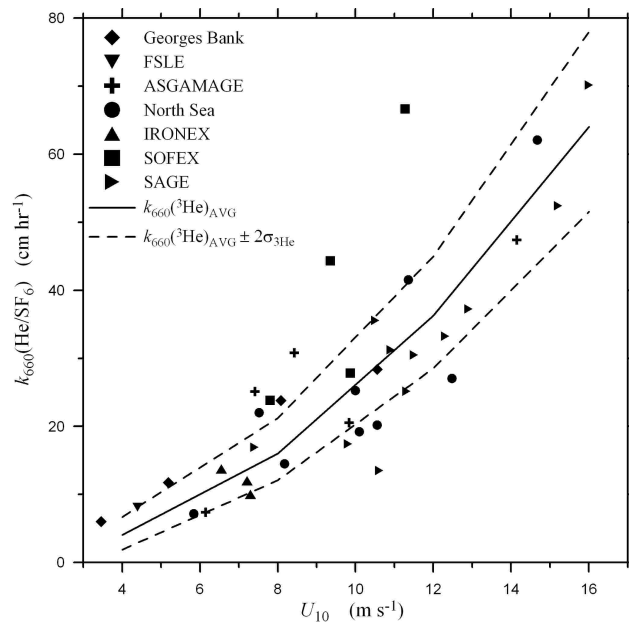


**Fig. 6.** Air-sea gas transfer velocities of helium-3 normalized to  $Sc=660$ ,  $k_{660}({}^3\text{He})$ , measured using the purposeful dual-tracer method (PDTM). Also shown are  $k_{660}({}^3\text{He})$  values produced by the Monte Carlo simulations described in Sect. 4. The data key is shown on the figure. Refer to the caption of Fig. 1 for explanation of experimental codes.

## Experimental error and air-sea gas exchange

W. E. Asher

Title Page

Abstract

Introduction

Conclusions

References

Tables

Figures

◀

▶

◀

▶

Back

Close

Full Screen / Esc

Printer-friendly Version

Interactive Discussion

